Progress In Electromagnetics Research C, Vol. 68, 85–93, 2016

Circularly Polarized Substrate Integrated Waveguide Cavity-Backed Antenna with Enhanced Bandwidth for Wideband Wireless Applications

Tian Li[1, *], Fu-Shun Zhang[1], Fei Gao[2], and Yan-Li Guo[3]

Abstract—A circularly polarized substrate integrated waveguide (SIW) cavity-backed antenna with the feasibility of obtaining a wide bandwidth is proposed and demonstrated. Fed by a modified inverted-T stripline, the proposed double-layered stacked antenna, consisting of an improved circular SIW cavity and a conventional perturbed circular patch radiator, is designed, analyzed and fabricated. Good agreement between simulated and measured results is observed. Simulation and measurement results reveal that the proposed antenna can provide an impedance bandwidth of 22.1% (4.94–6.17 GHz) and a 3-dB axial ratio (AR) bandwidth of 18.7% (5–6.03 GHz). Additionally, within the effective circular polarization (CP) bandwidth of 18.7% (5–6.03 GHz), the proposed antenna has gains from 4.3 dBic to 7.1 dBic with an average gain of 5.9 dBic. The measured CP bandwidth of 18.7% (5–6.03 GHz) not only meets the need for certain Wi-Fi (5.2/5.8 GHz) or WiMAX (5.5 GHz) band communication application, but also provides the potential to implement multiservice transmission.

1. INTRODUCTION

Circularly polarized substrate integrated waveguide (SIW) cavity-backed antennas have attracted great attention due to their merits of simplicity in structure, low profile, light weight, low fabrication cost, low loss, mitigating the effect of the unexpected electromagnetic interference in the installment environment due to self-consistent electrical shielding, realizing unidirectional radiation with higher gain, capabilities of reducing polarization mismatch, suppressing multipath interference, and suitability for integration with microwave circuits [1–12]. Meanwhile, though the feature of broad 3-dB axial ratio (AR) bandwidth is becoming increasingly necessary due to the high data rate required by modern services, many newly published circularly polarized SIW cavity-backed antennas in [5–8] only support narrow-band applications due to the inherent high-quality factor of the backed SIW cavities. In [5], a planar high-gain circularly polarized element antenna with an effective CP bandwidth of 0.99% is investigated for the use in array applications. Meanwhile, a dual-mode SIW cavity is utilized as the planar-backed cavity for the proposed antenna. In [6], a new low-profile circularly polarized hybrid antenna with an effective CP bandwidth of 1% is introduced. The proposed antenna consists of two resonators including semi-circular SIW cavity and patch antenna, which are coupled by proximity effect. In [7], a compact and circularly polarized planar antenna with an effective CP bandwidth of 5.8% is presented based on a quarter-mode substrate integrated waveguide sub-array. In [8], a single fed low-profile cavity-backed planar slot antenna for right handed circular polarization (RHCP) applications is first introduced by half mode substrate integrated waveguide (HMSIW) technique, which obtains an effective CP bandwidth of 1.74%. Furthermore, in [9], a traditional truncated corner patch antenna using annular gap and parallel

Received 11 July 2016, Accepted 21 September 2016, Scheduled 10 October 2016

* Corresponding author: Tian Li (tianli@stu.xidian.edu.cn).

[1] National Key Laboratory of Antennas and Microwave Technology, Xidian University, Xi'an 710071, China. [2] Electrical and Computer Engineering Department, University of California at San Diego, La Jolla, USA. [3] Institute of Science, Air Force Engineering University, Xi'an 710077, China.

plate capacitors with a foam substrate achieves an effective CP bandwidth of 12.6% around 2.4 GHz, with the cost of higher profile of 20 mm ($0.16\lambda_0$). In addition, for a conventional cavity-backed antenna, the height of the metallic cavity is inclined to be approximately a quarter-wavelength to support its radiation modes. As presented in [10], the proposed conventional cavity-backed antenna obtains a wide effective CP bandwidth of 43.3%, whereas its profile of 15 mm ($0.3\lambda_0$) is very high. In [11], an X-band circular polarized split-ring-slot SIW back-cavity antenna is proposed with an effective CP bandwidth of 1.72%, while its size is very compact.

In this paper, a relatively low-profile circularly polarized SIW cavity-backed antenna with an effective CP bandwidth of 18.7% is presented. Fed by a stripline, the proposed double-layered stacked antenna is based on a circular SIW cavity and a conventional perturbed circular patch mainly accounts for its CP radiation. Utilizing a modified inverted-T stripline with tapered structure, the axial ratio (AR) bandwidth can be greatly enhanced. To further enhance the AR performance, two sets of air vias are symmetrically loaded along two diagonals of the proposed antenna. Finally, a parasitic ring slot is etched on the upper metal layer of the SIW cavity to further improve the AR performance. For demonstration, the proposed antenna is fabricated and measured. The measured results have a reasonable agreement with the simulated ones.

2. ANTENNA CONFIGURATION

Figure 1 shows the configurations of the proposed double-layered stacked circularly polarized SIW cavity-backed antenna, which includes the front view of upper layer, the front view of lower layer, the back view of lower layer, the side view of upper and lower layers and the overall three-dimensional view of the proposed antenna. Both the upper and lower square substrate are with relative dielectric constant of 2.65, loss tangent of 0.0015 and surface area size of $L1 \times W1$ (64.2 mm $\times$ 73.4 mm). And they are $H1$ (3 mm) and $H2$ (2 mm) in height, respectively. A circular cavity with radius of $R4$ (26.4 mm) is produced by an annular array composed of 43 metallic vias with diameter of $2 * R7$ (1.8 mm) and distance of 3.68 mm penetrating through the proposed double-layered stacked antenna. Then a circular slot with radius of $R6$ (17.8 mm) is etched on the upper metal layer of the SIW cavity for the perturbed circular patch. The annular slot between the perturbed circular patch and the SIW cavity is $R6 - R3$

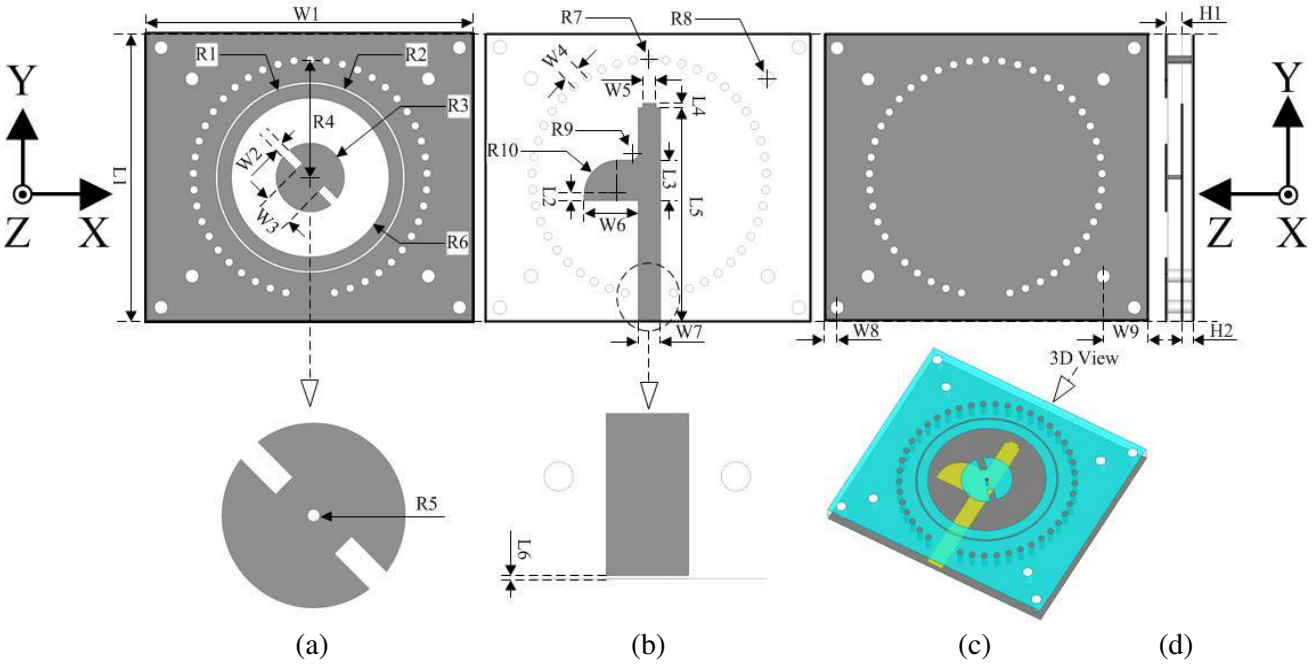

Figure 1. Configurations of the proposed antenna. (a) Front view of upper layer; (b) front view of lower layer; (c) back view of lower layer and 3D view; (d) side view of upper and lower layers.

(10.1 mm) in width. Two rectangular slots loaded at the upper left and lower right corners along the $-45°$ direction with reference to $+X$-axis act as a perturbation structure to yield right-hand circular polarization. The circular patch radiator is fed by an inverted-T stripline protruded into the SIW cavity, and they are connected by a metallic via with a radius of $R5$ (0.5 mm). The via locates in the center of the proposed antenna. Meanwhile, the distance of the via from the feeding end of the stripline is $L1/2 - L6$ (31.9 mm). To enhance the AR bandwidth, the inverted-T stripline etched on the front side of the lower substrate utilizes tapered and stepped structures at its two ends respectively. Meanwhile, since the stripline has a larger width of $W7$ (5.1 mm), a rectangular slot of $W7 \times L6$ (5.1 mm $\times$ 0.2 mm) is etched on the feeding end of the stripline acting as an isolation structure for welding convenience. Furthermore, two sets of air vias with radii of $R8$ (1.5 mm) are symmetrically loaded along two diagonals of the proposed antenna so as to further enhance the AR bandwidth. Moreover, these eight air vias also act as locating structures for the proposed double-layered stacked antenna, which facilitate the proposed antenna's installation and welding. Finally, a parasitic ring slot is etched on the upper metal layer of the SIW cavity to further improve the AR performance and its width is $R2 - R1$ (0.5 mm). The detailed geometry and dimensions of the proposed antenna are shown in Figure 1 and Table 1 after optimization using ANSYS HFSS.

Table 1. Dimensions of the proposed antenna.

Parameter	Value (mm)	Parameter	Value (mm)	Parameter	Value (mm)
$L1$	64.2	$W4$	3.68	$R4$	26.4
$L2$	1.3	$W5$	3	$R5$	0.5
$L3$	9	$W6$	12.15	$R6$	17.8
$L4$	1	$W7$	5.1	$R7$	0.9
$L5$	47.7	$W8$	3	$R8$	1.5
$L6$	0.2	$W9$	10	$R9$	1.5
$W1$	73.4	$R1$	20.9	$R10$	7.7
$W2$	2	$R2$	21.4	$H1$	3
$W3$	7	$R3$	7.7	$H2$	2

The proposed double-layered stacked circularly polarized SIW cavity-backed antenna employs indirect stripline-to-SIW feeding transition structure, hereby exciting the perturbed circular patch radiator with proximity coupling method, thus effectively enhancing its bandwidth. Meanwhile, multiple resonances of CP modes are generated by the perturbed circular patch radiator, the SIW cavity resonator and the annular slot resonator. When discreetly tuning their dimensions to make these resonances properly close to each other, the antenna bandwidth will be effectively broadened. Furthermore, the horizontal portion of the inverted-T stripline employs tapered structure to introduce extra asymmetry in feeding structure, which significantly enhances the AR bandwidth of the proposed antenna [13–15]. Moreover, by loading eight air vias along two diagonals of the proposed antenna, the effective dielectric constant of the substrates will be lowered, especially for the regions adjacent to the loaded air vias, which effectively enhance the AR bandwidth at upper frequencies, without affecting the AR performance in lower and middle frequencies [16]. In addition, a parasitic ring slot is etched on the upper metal layer of the SIW cavity as a perturbation structure to further improve the AR performance, especially for upper frequencies.

Figure 2 shows the simulated surface vector current distributions on the perturbed circular patch at 5.5 GHz viewed in $+Z$ ($\theta = 0°$) direction for different time phases of 0°, 90°, 180° and 270°, respectively. The surface current with red color refers to the dominant surface current. When the phase is equal to $0°/90°/180°/270°$, the dominant surface current is in the $-135°/-45°/45°/135°$ direction with reference to $+X$-axis. In other words, after one quarter-period, the current vector at 5.5 GHz rotates in the right-hand direction by 90° when viewed in $+Z$ direction, which satisfies the requirement of spatial/temporal quadrature for circular polarization.

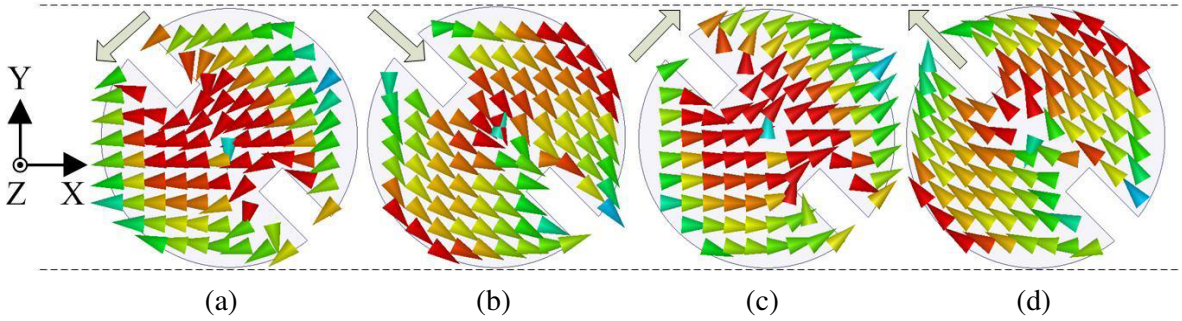

Figure 2. Simulated surface vector current distributions of the perturbed circular patch radiator at 5.5 GHz for four phases. (a) 0°, (b) 90°, (c) 180°, (d) 270°.

3. CHOICE OF THE PARAMETERS

All critical physical parameters, such as $R3$, $W2$, $W3$, $R4$, $R6$, $R10$, $R8$ and $R1$, should be adjusted carefully to achieve a good performance. During this process, all the other parameters not mentioned stay constant as shown in Table 1.

3.1. Effect of Perturbed Circular Patch Radiator ($R3$, $W2$ and $W3$)

The effects of the perturbed circular patch radiator on the impedance and AR bandwidths are shown in Figure 3, Figure 4 and Figure 5, respectively. As expected, as $R3$ increases, the whole operating band shifts toward lower band. Meanwhile, compared to the impedance performance, the AR performance is much more sensitive to varied $R3$. Moreover, as $W2$ and $W3$ vary, the AR bandwidth at both lower and upper frequencies will be affected, especially for lower frequencies, while it has little influence on the impedance bandwidth. To obtain good impedance matching and AR performance, $R3$, $W2$ and $W3$ are set as 7.7 mm, 2 mm and 7 mm, respectively.

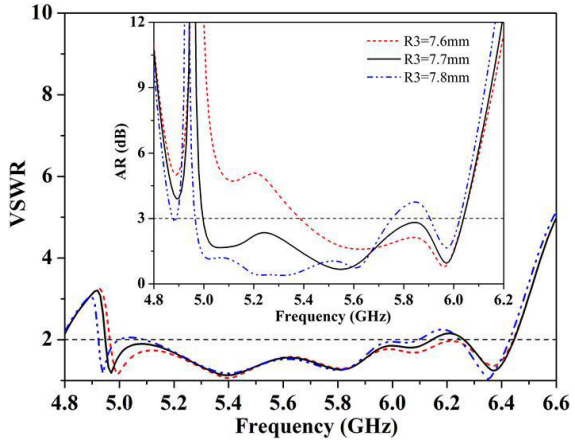

Figure 3. VSWRs and ARs with varied $R3$.

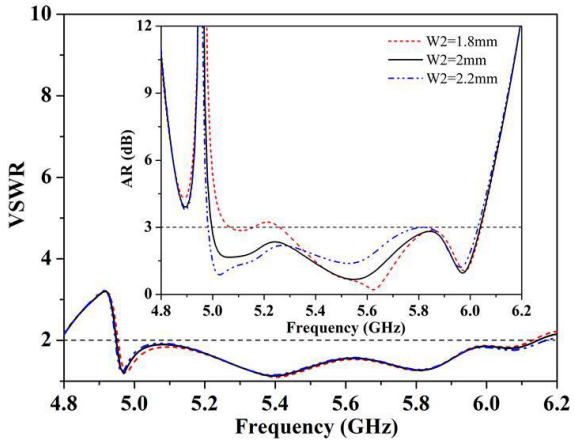

Figure 4. VSWRs and ARs with varied $W2$.

3.2. Effect of SIW Cavity and Annular Slot ($R4$ and $R6$)

Figure 6 and Figure 7 reveal the influence of the SIW cavity and the annular slot on the impedance and AR bandwidths, respectively. As $R4$/$R6$ increases/decreases, the whole impedance bandwidth shifts toward lower band. While the AR bandwidth will be deteriorated, whether the values of $R4$ and $R6$ increases or decreases. Thus, the performance in AR bandwidth is very sensitive to the radii of the

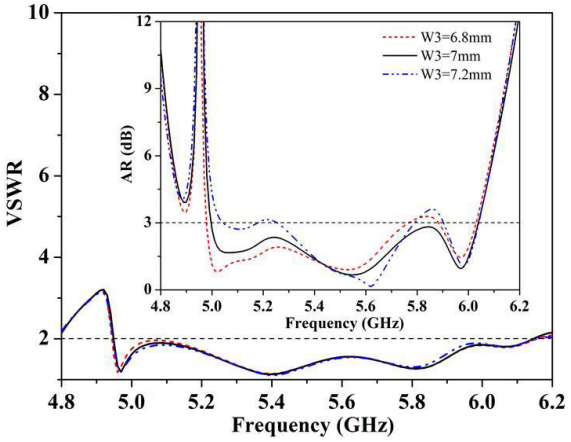

Figure 5. VSWRs and ARs with varied $W3$.

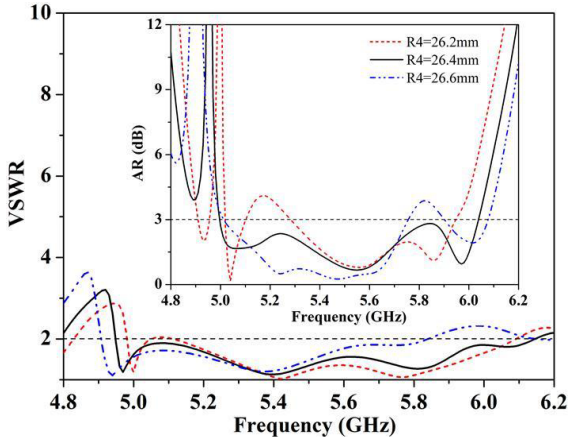

Figure 6. VSWRs and ARs with varied $R4$.

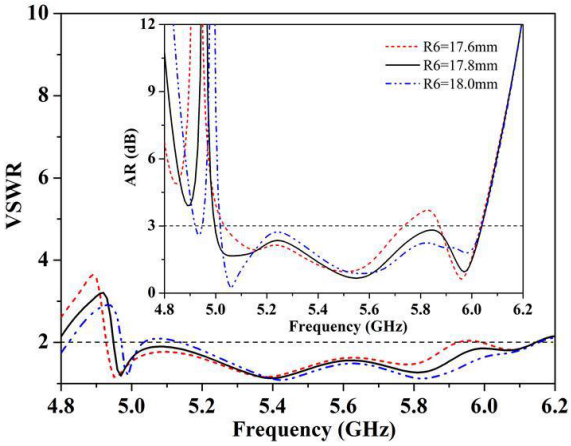

Figure 7. VSWRs and ARs with varied $R6$.

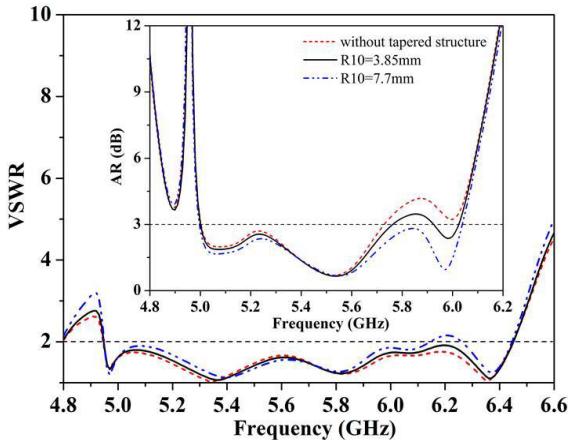

Figure 8. VSWRs and ARs with varied $R10$.

circular SIW cavity and the annular slot. To obtain good impedance matching and AR performance, $R4$ and $R6$ are carefully tuned as 26.4 mm and 17.8 mm, respectively.

3.3. Effect of Inverted-T Stripline, Air Vias and Ring Slot ($R10$, $R8$ and $R1$)

The effects of the inverted-T stripline, air vias and ring slot on the impedance and AR bandwidths are shown in Figure 8, Figure 9 and Figure 10, respectively. As $R10$ increases, the AR bandwidth at upper frequencies will be significantly enhanced, while the impedance performance almost stays the same. Hence, with this tapered structure for the inverted-T stripline, the AR bandwidth of the proposed antenna is greatly enhanced, without significant degradation in impedance performance. Furthermore, as $R8$ increases, the AR bandwidth at upper frequencies will be effectively enhanced while the impedance performance almost stays the same. Consequently, the presence of these air vias effectively improves the antenna performance. In addition, as shown in Figure 10, without the ring slot loaded on the upper metal layer of the SIW cavity, the values of AR for some frequencies within upper operating frequency band are slightly greater than 3 dB. When the ring slot is introduced with discreetly optimized width of 0.5 mm, the AR performance at these frequencies will be effectively improved.

On the basis of the parametric study for these eight critical physical parameters, the optimal values of these eight parameters chosen for the prototype, namely $R3$, $W2$, $W3$, $R4$, $R6$, $R10$, $R8$ and $R1$, are 7.7 mm, 2 mm, 7 mm, 26.4 mm, 17.8 mm, 7.7 mm, 1.5 mm and 20.9 mm, respectively. Meanwhile, the effects of these parameters on impedance and AR bandwidths are examined above in detail to facilitate the design of a same or homogeneous antenna with different specifications.

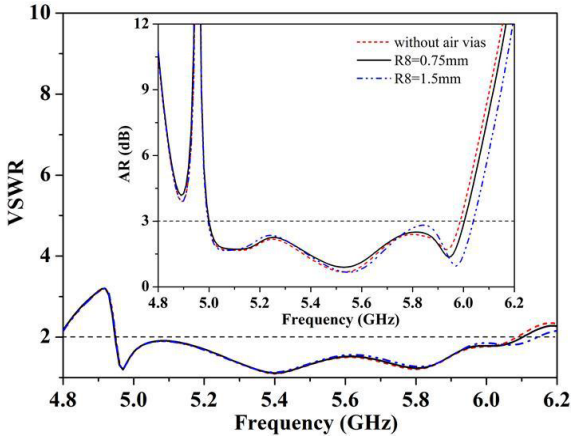

Figure 9. VSWRs and ARs with varied $R8$.

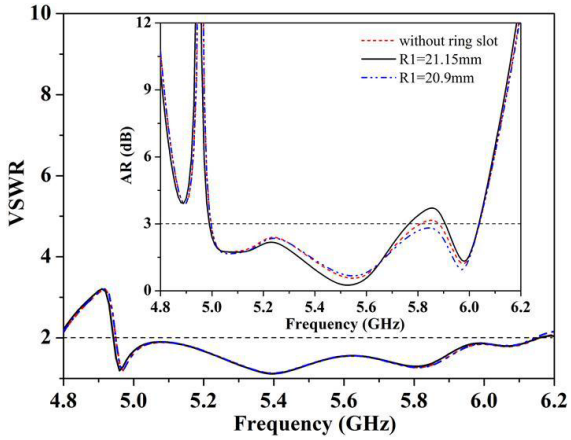

Figure 10. VSWRs and ARs with varied $R1$.

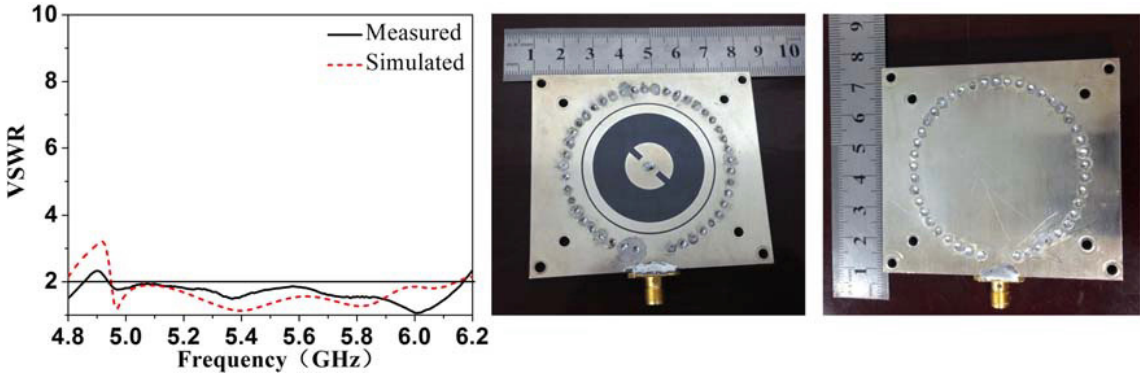

Figure 11. Simulated and measured VSWRs and the photographs of the fabricated antenna. (a) VSWRs; (b) front view of the fabricated antenna; (c) back view of the fabricated antenna.

4. RESULTS

The measured and simulated VSWRs of the proposed antenna are depicted in Figure 11. Good agreement between the simulated and measured results is obtained. With reference to the figure, the simulated and measured impedance bandwidths (VSWR $\leq$ 2) of the proposed antenna are 21.6% (4.95–6.15 GHz) and 22.1% (4.94–6.17 GHz), respectively.

Figure 12 shows the simulated and measured radiation patterns in the XZ-planes ($\varphi = 0°$) and YZ-planes ($\varphi = 90°$) at 5, 5.5 and 6 GHz. The radiation patterns are not symmetry, especially for the higher frequencies. This is mainly due to the asymmetrical design of the proposed antenna's structure. Meanwhile, the relatively higher back lobes are mainly caused by the limited ground plane size, especially for the lower frequencies. In Figure 13, the measured gains are from 4.3 dBic to 7.1 dBic with an average gain of 5.9 dBic. Meanwhile, the simulated and measured 3-dB AR bandwidths (AR $\leq$ 3) are 18.8% (5–6.04 GHz) and 18.7% (5–6.03 GHz), respectively. It should be noted that the discrepancy between the simulated and measured results may be caused by the imperfect testing environment, which is mainly due to the interferences from indoor reflection. Furthermore, the errors in the process of fabrication, namely the errors resulted from limited processing accuracy and the errors of un-uniformity of the substrate with respect to relative dielectric constant and loss tangent, and the presence of the SMA connector interfering with the radiated field may be taken into account as well. In addition, the measured effective CP bandwidth of 18.7% (5–6.03 GHz) not only includes certain Wi-Fi (5.2/5.8 GHz) or WiMAX

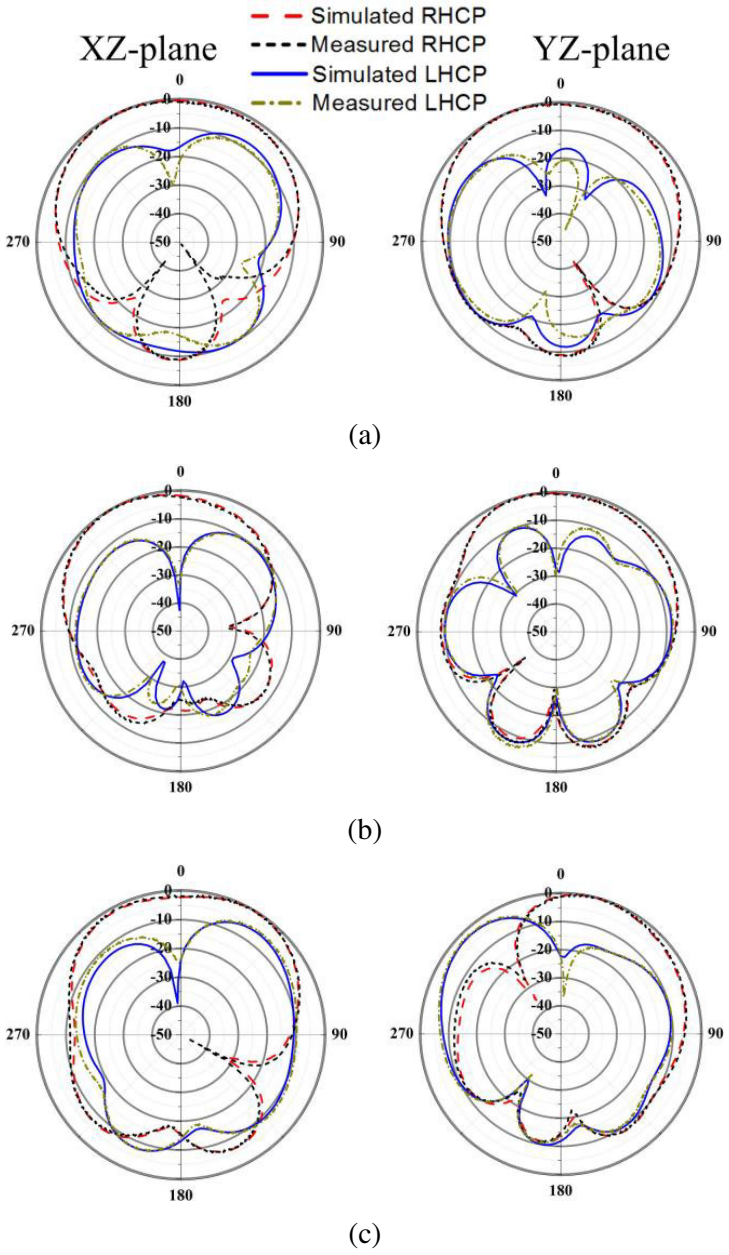

Figure 12. Simulated and measured normalized radiation patterns in the XZ-plane ($\varphi = 0°$) and YZ-plane ($\varphi = 90°$). (a) 5 GHz; (b) 5.5 GHz; (c) 6 GHz.

(5.5 GHz) band communication application, but also offers the potential to implement multiservice transmission.

A comparison of the proposed antenna with previous work is made in terms of effective CP bandwidth, antenna substrate relative dielectric constant, antenna height and peak gain with results presented in Table 2. The selection criteria for inclusion in this comparison are newly published unidirectional CP antennas. From Table 2, it could be seen that the proposed antenna provides either a lower profile or a wider effective CP bandwidth. Actually, it obtains a better performance with a favorable compromise between operating bandwidth and antenna profile.

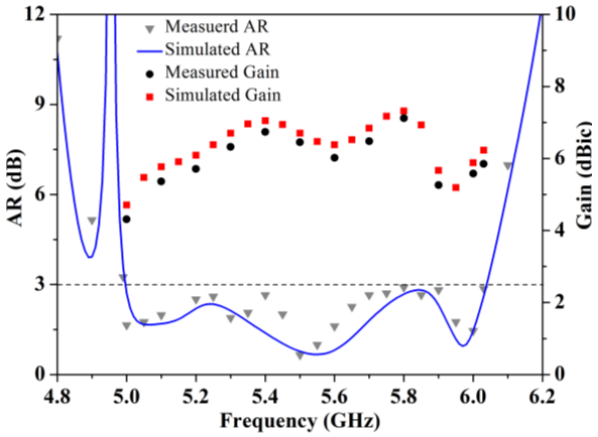

Figure 13. Simulated and measured ARs and gains of the proposed antenna.

Table 2. Performance comparisons between the proposed and referenced antennas.

Reference Designs	BW (GHz)	Substrate ε_r	Antenna Height (mm)	Peak Gain (dBic)
Proposed Antenna	5–6.03 (18.7%)	2.65	5 ($0.09\lambda_0$)	7.1 dBic at 5.8 GHz
Hao et al. [5]	6.55–6.615 (0.99%)	2.2	1.57 ($0.03\lambda_0$)	9.6 dBic at 6.57 GHz
Dashti et al. [6]	7.94–8.02 (1%)	2.2	0.787 ($0.02\lambda_0$)	6.8 dBic
Jin et al. [7]	5.02–5.32 (5.8%)	2.2	1.57 ($0.03\lambda_0$)	5.58 dBic at 5.2 GHz
Razavi et al. [8]	8.65–8.8 (1.74%)	2.2	0.78 ($0.02\lambda_0$)	4.87 dBic
Kovitz et al. [9]	12.6% around 2.4 GHz	1	20 ($0.16\lambda_0$)	Not mentioned
Yang et al. [10]	4.8–7.4 (43.3%)	4.4/2.55	15 ($0.3\lambda_0$)	8.6 dBic at 7.4 GHz

5. CONCLUSION

A circularly polarized SIW cavity-backed antenna with enhanced bandwidth has been presented. Simulation and measurement results indicate that with a modified inverted-T feeding stripline and an improved SIW cavity, the proposed double-layered stacked antenna can realize an impedance bandwidth of 22.1% (4.94–6.17 GHz) and a 3-dB AR bandwidth of 18.7% (5–6.03 GHz). The effects of all critical parameters on impedance and AR bandwidths are studied in detail to facilitate the design of a same or homogeneous antenna. Meanwhile, within the effective CP bandwidth of 18.7% (5–6.03 GHz), relatively moderate gains, ranging from 4.3 dBic to 7.1 dBic with an average gain of 5.9 dBic, are obtained simultaneously. With these inherent characteristics, the proposed antenna can be a good candidate for wideband wireless applications.

REFERENCES

1. Luo, G.-Q., Z.-F. Hu, Y.-P. Liang, L.-Y. Yu, and L.-L. Sun, "Development of low profile cavity backed crossed slot antennas for planar integration," *IEEE Trans. Antennas Propag.*, Vol. 57, No. 10, 2972–2979, Oct. 2009.
2. Kim, D.-Y., J.-W. Lee, and C.-S. Cho, "Design of SIW cavity-backed circular-polarized antennas using two different feeding transitions," *IEEE Trans. Antennas Propag.*, Vol. 59, No. 4, 1398–1403, Apr. 2011.
3. Zhou, H., W. Hong, L. Tian, and M. Jiang, "A polarization-rotating SIW reflective surface with two sharp band edges," *IEEE Antennas Wireless Propag. Lett.*, Vol. 15, 130–134, Feb. 2016.

4. Guan, D.-F., C. Ding, Z.-P. Qian, Y.-S. Zhang, Y.-J. Guo, and K. Gong, "Broadband high-gain SIW cavity-polarized array antenna," *IEEE Trans. Antennas Propag.*, Vol. 64, No. 4, 1493–1496, Apr. 2016.
5. Hao, Z.-C., X.-M. Liu, T. Ni, X.-P. Huo, and K.-K. Fan, "Planar high-gain circularly polarized element antenna for array applications," *IEEE Trans. Antennas Propag.*, Vol. 63, No. 5, 1937–1948, May 2015.
6. Dashti, H. and M.-H. Neshati, "Development of low-profile patch and semi-circular SIW cavity hybrid antennas," *IEEE Trans. Antennas Propag.*, Vol. 62, No. 9, 4481–4488, Sep. 2014.
7. Jin, C., Z.-X. Shen, R. Li, and A. Alphones, "Compact circularly polarized antenna based on quarter-mode substrate integrated waveguide sub-array," *IEEE Trans. Antennas Propag.*, Vol. 62, No. 2, 963–967, Feb. 2014.
8. Razavi, S.-A. and M.-H. Neshati, "Development of a low-profile circularly polarized cavity-backed antenna using HMSIW technique," *IEEE Trans. Antennas Propag.*, Vol. 61, No. 3, 1041–1047, Mar. 2013.
9. Kovitz, J.-M. and Y. Rahmat-Sammi, "Using thick substrates and capacitive probe compensation to enhance the bandwidth of traditional CP patch antennas," *IEEE Trans. Antennas Propag.*, Vol. 62, No. 10, 4970–4979, Oct. 2014.
10. Yang, W.-W. and J.-Y. Zhou, "Wideband circularly polarized cavity-backed aperture antenna with a parasitic square patch," *IEEE Antennas Wireless Propag. Lett.*, Vol. 13, 197–200, Feb. 2014.
11. Huang, J.-Q., F. Qiu, C. Jiang, D. Lei, Z. Tang, M. Yao, and Q.-X. Chu, "Compact coaxial probe-fed CP substrate integrated waveguide cavity-backed antenna utilizing slot split ring," *Progress In Electromagnetics Research Letters*, Vol. 60, 107–112, 2016.
12. Lacik, J., "Circularly polarized SIW square ring-slot antenna for X-band applications," *Microwave Opt. Technol. Lett.*, Vol. 54, No. 11, 2590–2594, Nov. 2012.
13. Thomas, K.-G. and G. Praveen, "A novel wideband circularly polarized printed antenna," *IEEE Trans. Antennas Propag.*, Vol. 60, No. 12, 5564–5570, Dec. 2012.
14. Tran, H.-H. and I. Park, "Wideband circularly polarized cavity-backed asymmetric crossed bowtie dipole antenna," *IEEE Antennas Wireless Propag. Lett.*, Vol. 15, 358–361, Feb. 2016.
15. Han, R.-C. and S.-S. Zhong, "Broadband circularly-polarised chifre-shaped monopole antenna with asymmetric feed," *IET Electron. Lett.*, Vol. 52, No. 4, 256–258, Feb. 2016.
16. Cai, Y., Y.-S. Zhang, Z.-P. Qian, W.-Q. Cao, and L. Wang, "Design of compact air-vias-perforated SIW horn antenna with partially detached broad walls," *IEEE Trans. Antennas Propag.*, Vol. 64, No. 6, 2100–2107, Jun. 2016.